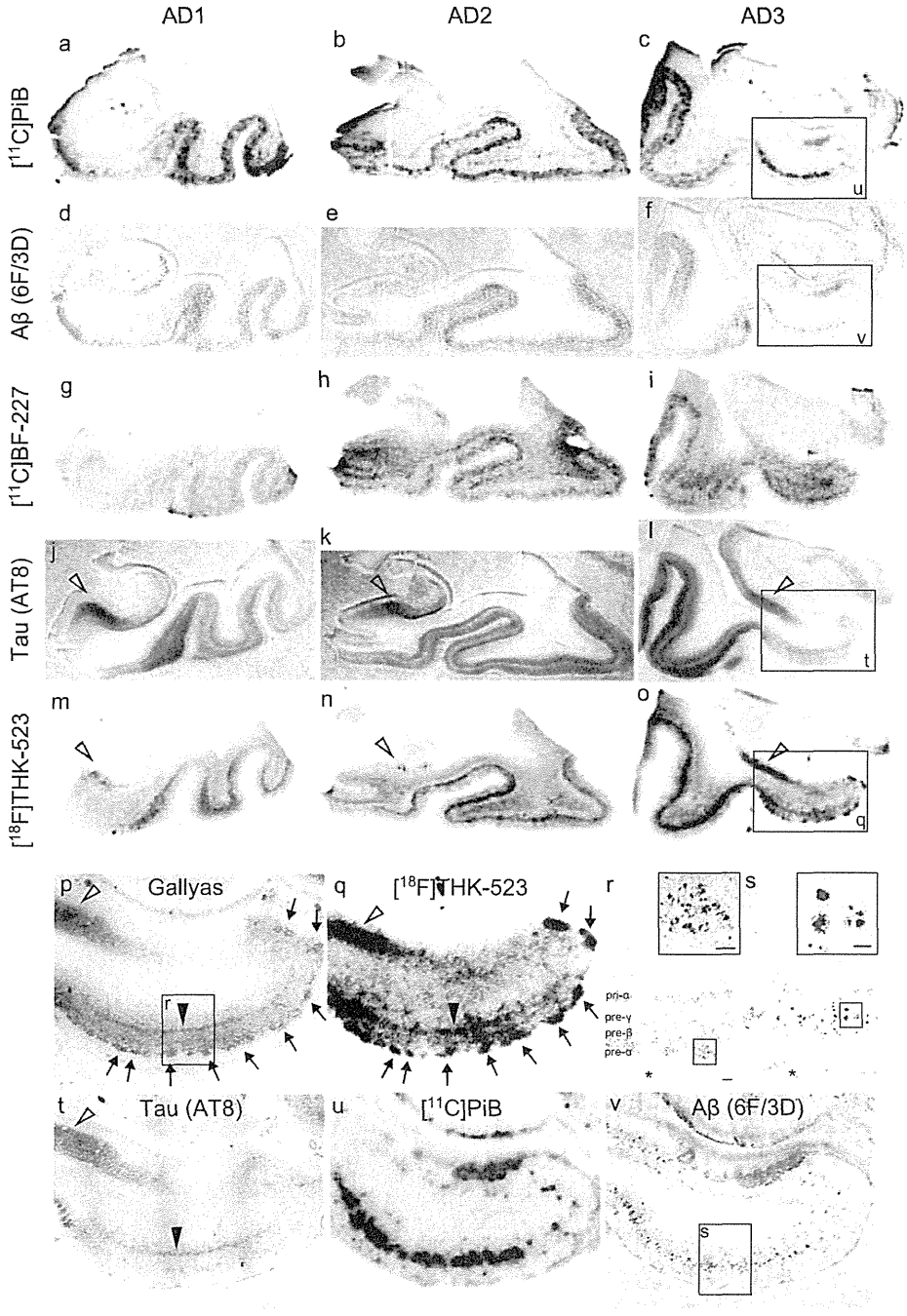

Fig. 3 Comparison of [^{11}C]PiB, [^{11}C]BF-227 and [^{18}F]THK-523 autoradiography with Aβ and tau immunostaining images in sections of the medial temporal brain from three patients with AD (*AD1*, *AD2*, *AD3*). [^{11}C]PiB (**a**–**c**) and [^{11}C]BF-227 (**g**–**i**) do not accumulate in the hippocampal CA1 area which contains a low density of Aβ (**d**–**f**). In contrast, accumulation of [^{18}F]THK-523 is observed in the hippocampal CA1 area (**m**–**o**, *arrowheads*), which closely resembles AT8 immunoreactivity (**j**–**l**, *arrowheads*). In addition, the band-like labelling pattern of [^{18}F]THK-523 in the inner layer of temporal cortex (**m**–**o**) is closely similar to that of AT8 immunostaining (**j**–**l**). **p**–**v** High magnification images of the medial temporal sections from patient AD3. Many clusters of [^{18}F]THK-523 binding in the ERC are consistent with Gallyas silver staining (**p**, **q**, *arrows*). **r** Close-up image from **p**. Numerous NFTs are located in the layer pre-α of the ERC (**r** *inset*). The band-like distribution of [^{18}F]THK-523 in the layer pri-α of the ERC also resembles the labelling pattern of Gallyas silver staining (**p**, *filled arrowhead*) as well as AT8 immunoreactivity (**t**, *filled arrowhead*). [^{11}C]PiB binding (**u**) is also present in the ERC, but obviously different from [^{18}F]THK-523 binding (**q**) and similar to the 6F/3D immunostaining pattern (**v**). Lake-like amyloid in the presubicular region (**v**) is labelled with [^{11}C]PiB, but not with [^{18}F]THK-523. **s** Close-up image from **v**. Aβ plaques (**s** *inset*) located in the layer pre-β and pre-γ are intensely labelled with [^{11}C]PiB (**u**). *Asterisks* in **r** and **s** denote the same large blood vessel. *Scale bar* 100 μm

plaque-free and NFT-rich ERC homogenates, despite the high amount of [^{3}H]BTA-1 binding to frontal cortex homogenates containing high levels of neuritic plaques [30]. Autoradiographic and immunohistochemical analyses indicated that PiB predominantly binds to senile plaques but not to NFTs. These findings are consistent with the findings from clinical PiB-PET studies showing no remarkable PiB retention in the medial temporal cortex of AD patients [7].

Another radiotracer, [^{18}F]FDDNP, has been reported to detect Aβ and tau pathological lesions in AD patients [3]. Previous clinical PET studies have shown higher cortical uptake of [^{18}F]FDDNP in the lateral and medial temporal lobes of AD subjects [3, 5]. Furthermore, a multitracer PET study of [^{11}C]PiB and [^{18}F]FDDNP has shown significant retention of FDDNP in the medial temporal cortex, albeit no remarkable retention of PiB in the same region [31]. However, in vitro binding studies have shown the limited binding affinity of [^{3}H]FDDNP to AD pathological lesions [24], and a previous autoradiographic analysis has suggested that [^{3}H]FDDNP does not significantly label any region in AD brain [24]. Previous in vitro binding studies additionally showed the binding affinity of FDDNP for $A\beta_{40}$ fibrils (K_D 0.12, 85 nM) [19, 24], but the binding affinity for tau fibrils was not reported. Here, we showed that the binding affinity of [^{18}F]FDDNP for tau fibrils (K_{D1} 36.7 nM) was similar to that of [^{18}F]BF-227 (K_{D1} 30.2 nM), but much higher than that of [^{18}F]THK-523 (K_{D1} 1.99 nM).

In conclusion, the binding profiles of [^{18}F]THK-523, [^{11}C]PiB, [^{18}F]BF-227, and [^{18}F]FDDNP were compared using in vitro saturation binding assays and autoradiography of sections of AD brain. These data suggest that [^{18}F]THK-523 shows a binding preference for tau protein fibrils. Therefore, [^{18}F]THK-523 is a candidate as a radiotracer to identify tau protein deposits and a lead compound for future tracer development. Ongoing clinical trials will clarify the clinical utility of this tracer and its derivatives for tau imaging in vivo.

Acknowledgments This study was supported by the Industrial Technology Research Grant Program of the NEDO in Japan, Health and Labor Sciences Research Grants from the Ministry of Health, Labor, and Welfare of Japan, and Grant-in-Aid for Scientific Research (B) (23390297).

References

1. Nordberg A, Rinne JO, Kadir A, Langstrom B. The use of PET in Alzheimer disease. Nat Rev Neurol. 2010;6:78–87. doi:10.1038/nrneurol.2009.217.
2. Furumoto S, Okamura N, Iwata R, Yanai K, Arai H, Kudo Y. Recent advances in the development of amyloid imaging agents. Curr Top Med Chem. 2007;7:1773–89.
3. Shoghi-Jadid K, Small GW, Agdeppa ED, Kepe V, Ercoli LM, Siddarth P, et al. Localization of neurofibrillary tangles and beta-amyloid plaques in the brains of living patients with Alzheimer disease. Am J Geriatr Psychiatry. 2002;10:24–35.
4. Mathis CA, Wang Y, Holt DP, Huang GF, Debnath ML, Klunk WE. Synthesis and evaluation of 11C-labeled 6-substituted 2-arylbenzothiazoles as amyloid imaging agents. J Med Chem. 2003;46:2740–54. doi:10.1021/jm030026b.
5. Klunk WE, Engler H, Nordberg A, Wang Y, Blomqvist G, Holt DP, et al. Imaging brain amyloid in Alzheimer's disease with Pittsburgh Compound-B. Ann Neurol. 2004;55:306–19. doi:10.1002/ana.20009.
6. Kudo Y, Okamura N, Furumoto S, Tashiro M, Furukawa K, Maruyama M, et al. 2-(2-[2-Dimethylaminothiazol-5-yl]ethenyl)-6- (2-[fluoro]ethoxy)benzoxazole: a novel PET agent for in vivo detection of dense amyloid plaques in Alzheimer's disease patients. J Nucl Med. 2007;48:553–61.
7. Ikonomovic MD, Klunk WE, Abrahamson EE, Mathis CA, Price JC, Tsopelas ND, et al. Post-mortem correlates of in vivo PiB-PET amyloid imaging in a typical case of Alzheimer's disease. Brain. 2008;131:1630–45. doi:10.1093/brain/awn016.
8. Sperling RA, Aisen PS, Beckett LA, Bennett DA, Craft S, Fagan AM, et al. Toward defining the preclinical stages of Alzheimer's disease: recommendations from the National Institute on Aging-Alzheimer's Association workgroups on diagnostic guidelines for Alzheimer's disease. Alzheimers Dement. 2011;7:280–92. doi:10.1016/j.jalz.2011.03.003.
9. Jack Jr CR, Knopman DS, Jagust WJ, Shaw LM, Aisen PS, Weiner MW, et al. Hypothetical model of dynamic biomarkers of the Alzheimer's pathological cascade. Lancet Neurol. 2010;9:119–28. doi:10.1016/S1474-4422(09)70299-6.
10. Pike KE, Savage G, Villemagne VL, Ng S, Moss SA, Maruff P, et al. Beta-amyloid imaging and memory in non-demented individuals: evidence for preclinical Alzheimer's disease. Brain. 2007;130:2837–44. doi:10.1093/brain/awm238.
11. Okamura N, Suemoto T, Furumoto S, Suzuki M, Shimadzu H, Akatsu H, et al. Quinoline and benzimidazole derivatives: candidate probes for in vivo imaging of tau pathology in Alzheimer's disease. J Neurosci. 2005;25:10857–62. doi:10.1523/JNEUROSCI.1738-05.2005.
12. Fodero-Tavoletti MT, Okamura N, Furumoto S, Mulligan RS, Connor AR, McLean CA, et al. 18F-THK523: a novel in vivo tau imaging ligand for Alzheimer's disease. Brain. 2011;134:1089–100. doi:10.1093/Brain/Awr038.
13. Lockhart A, Lamb JR, Osredkar T, Sue LI, Joyce JN, Ye L, et al. PIB is a non-specific imaging marker of amyloid-beta (Abeta) peptide-related cerebral amyloidosis. Brain. 2007;130:2607–15. doi:10.1093/brain/awm191.
14. Burack MA, Hartlein J, Flores HP, Taylor-Reinwald L, Perlmutter JS, Cairns NJ. In vivo amyloid imaging in autopsy-confirmed Parkinson disease with dementia. Neurology. 2010;74:77–84. doi:10.1212/WNL.0b013e3181c7da8e.
15. Clark CM, Schneider JA, Bedell BJ, Beach TG, Bilker WB, Mintun MA, et al. Use of florbetapir-PET for imaging beta-amyloid pathology. JAMA. 2011;305:275–83. doi:10.1001/jama.2010.2008.
16. Wong DF, Moghekar AR, Rigamonti D, Brasic JR, Rousset O, Willis W, et al. An in vivo evaluation of cerebral cortical amyloid with [(18)F]Flutemetamol using positron emission tomography compared with parietal biopsy samples in living normal pressure hydrocephalus patients. Mol Imaging Biol. 2012. doi:10.1007/s11307-012-0583-x.
17. Maeda J, Ji B, Irie T, Tomiyama T, Maruyama M, Okauchi T, et al. Longitudinal, quantitative assessment of amyloid, neuroinflammation, and anti-amyloid treatment in a living mouse model of Alzheimer's disease enabled by positron emission tomography. J Neurosci. 2007;27:10957–68. doi:10.1523/JNEUROSCI.0673-07.2007.

18. Manook A, Yousefi BH, Willuweit A, Platzer S, Reder S, Voss A, et al. Small-animal PET imaging of amyloid-beta plaques with [11C]PiB and its multi-modal validation in an APP/PS1 mouse model of Alzheimer's disease. PLoS One. 2012;7:e31310. doi:10.1371/journal.pone.0031310.
19. Agdeppa ED, Kepe V, Liu J, Flores-Torres S, Satyamurthy N, Petric A, et al. Binding characteristics of radiofluorinated 6-dialkylamino-2-naphthylethylidene derivatives as positron emission tomography imaging probes for beta-amyloid plaques in Alzheimer's disease. J Neurosci. 2001;21:RC189.
20. Gallyas F. Silver staining of Alzheimer's neurofibrillary changes by means of physical development. Acta Morphol Acad Sci Hung. 1971;19:1–8.
21. Barghorn S, Davies P, Mandelkow E. Tau paired helical filaments from Alzheimer's disease brain and assembled in vitro are based on beta-structure in the core domain. Biochemistry. 2004;43:1694–703. doi:10.1021/bi0357006.
22. von Bergen M, Barghorn S, Muller SA, Pickhardt M, Biernat J, Mandelkow EM, et al. The core of tau-paired helical filaments studied by scanning transmission electron microscopy and limited proteolysis. Biochemistry. 2006;45:6446–57. doi:10.1021/bi052530j.
23. Fodero-Tavoletti MT, Mulligan RS, Okamura N, Furumoto S, Rowe CC, Kudo Y, et al. In vitro characterisation of BF227 binding to alpha-synuclein/Lewy bodies. Eur J Pharmacol. 2009;617:54–8. doi:10.1016/j.ejphar.2009.06.042.
24. Thompson PW, Ye L, Morgenstern JL, Sue L, Beach TG, Judd DJ, et al. Interaction of the amyloid imaging tracer FDDNP with hallmark Alzheimer's disease pathologies. J Neurochem. 2009;109:623–30. doi:10.1111/j.1471-4159.2009.05996.x.
25. Braak E, Braak H, Mandelkow EM. A sequence of cytoskeleton changes related to the formation of neurofibrillary tangles and neuropil threads. Acta Neuropathol. 1994;87:554–67.
26. Thal DR, Rub U, Schultz C, Sassin I, Ghebremedhin E, Del Tredici K, et al. Sequence of Abeta-protein deposition in the human medial temporal lobe. J Neuropathol Exp Neurol. 2000;59:733–48.
27. Villemagne VL, Furumoto S, Fodero-Tavoletti M, Harada R, Mulligan RS, Kudo Y, et al. The challenges of tau imaging. Future Neurol. 2012;7:409–21. doi:10.2217/fnl.12.34.
28. Fodero-Tavoletti MT, Smith DP, McLean CA, Adlard PA, Barnham KJ, Foster LE, et al. In vitro characterization of Pittsburgh compound-B binding to Lewy bodies. J Neurosci. 2007;27:10365–71. doi:10.1523/JNEUROSCI.0630-07.2007.
29. Klunk WE, Lopresti BJ, Ikonomovic MD, Lefterov IM, Koldamova RP, Abrahamson EE, et al. Binding of the positron emission tomography tracer Pittsburgh compound-B reflects the amount of amyloid-beta in Alzheimer's disease brain but not in transgenic mouse brain. J Neurosci. 2005;25:10598–606. doi:10.1523/JNEUROSCI.2990-05.2005.
30. Klunk WE, Wang Y, Huang GF, Debnath ML, Holt DP, Shao L, et al. The binding of 2-(4'-methylaminophenyl)benzothiazole to post-mortem brain homogenates is dominated by the amyloid component. J Neurosci. 2003;23:2086–92.
31. Shin J, Lee SY, Kim SH, Kim YB, Cho SJ. Multitracer PET imaging of amyloid plaques and neurofibrillary tangles in Alzheimer's disease. Neuroimage. 2008;43:236–44. doi:10.1016/j.neuroimage.2008.07.022.

Insights Imaging
DOI 10.1007/s13244-014-0312-x

PICTORIAL REVIEW

Imaging spectrum of sporadic cerebral amyloid angiopathy: multifaceted features of a single pathological condition

Keita Sakurai · Aya M. Tokumaru · Tomoya Nakatsuka · Shigeo Murayama · Shin Hasebe · Etsuko Imabayashi · Kazutomi Kanemaru · Masaki Takao · Hiroyuki Hatsuta · Kenji Ishii · Yuko Saito · Yuta Shibamoto · Noriyuki Matsukawa · Emiko Chikui · Hitoshi Terada

Received: 14 July 2013 / Revised: 23 December 2013 / Accepted: 13 January 2014

Abstract
Objectives Sporadic cerebral amyloid angiopathy (CAA) is common cause of cerebrovascular disorders that predominantly affect elderly patients. When symptomatic, cortical-subcortical intracerebral haemorrhage (ICH) in the elderly is the most well-known manifestation of CAA. Furthermore, the clinical presentation varies from a sudden neurological deficit to seizures, transient symptoms and acute progressive cognitive decline. Despite its clinical importance, this multifaceted nature poses a diagnostic challenge for radiologists. The aims of this study were to expound the characteristics of neuroimaging modalities, which cover a wide spectrum of CAA-related imaging findings, and to review the various abnormal findings for which CAA could be responsible.
Conclusions Radiologically, in addition to typical ICH, CAA leads to various types of abnormal findings, including microbleed, subarachnoid haemorrhage, superficial siderosis, microinfarction, reversible oedema, and irreversible leukoaraiosis. Taking into consideration the clinical importance of CAA-related disorders such as haemorrhagic risks and treatable oedema, it is necessary for radiologists to understand the wide spectrum of CAA-related imaging findings.
Teaching Points
- *To describe the characteristics of imaging modalities and findings of CAA-related disorders.*
- *MRI, especially gradient echo sequences, provides the useful information of CAA-related haemosiderin depositions.*
- *To understand the wide spectrum of CAA-related neuroimaging and clinical features is important.*

Keywords Cerebral amyloid angiopathy · Imaging · Subarachnoid haemorrhage · Microbleed · Superficial siderosis · CAA-related inflammation

K. Sakurai (✉) · A. M. Tokumaru · S. Hasebe · E. Imabayashi
Department of Diagnostic Radiology, Tokyo Metropolitan Medical Centre of Gerontology, 35-2 Sakaecho, Itabashi-ku, Tokyo 173-0015, Japan
e-mail: ksak666@yahoo.co.jp

T. Nakatsuka · H. Terada
Department of Radiology, Toho University Sakura Medical Centre, Sakura, Japan

S. Murayama · M. Takao · H. Hatsuta
Department of Neuropathology (the Brain Bank for Aging Research), Tokyo Metropolitan Geriatric Hospital, Tokyo Metropolitan Geriatric Hospital and Institute of Gerontology, Tokyo, Japan

K. Kanemaru
Department of Neurology, Tokyo Metropolitan Geriatric Hospital, Tokyo, Japan

K. Ishii
Positron Medical Centre, Tokyo Metropolitan Institute of Gerontology, Tokyo, Japan

Y. Saito
Department of Pathology and Laboratory Medicine, National Centre for Neurology and Psychiatry Hospital, Tokyo, Japan

Y. Shibamoto
Department of Radiology, Nagoya City University Graduate School of Medical Sciences, Nagoya, Japan

N. Matsukawa
Department of Neurology and Neuroscience, Nagoya City University Graduate School of Medical Sciences, Nagoya, Japan

E. Chikui
Department of Neurosurgery, Tokyo Metropolitan Geriatric Hospital, Tokyo, Japan

Published online: 12 February 2014

Introduction

Sporadic cerebral amyloid angiopathy (CAA) is a common small vessel disease of the brain, characterised by the progressive deposition of amyloid-β (Aβ) protein in the walls of small- to medium-sized arteries (up to about 2 mm in diameter), arterioles and capillaries in the cerebral cortex and overlying leptomeninges, preferentially affecting occipital regions for unclear reasons. In contrast to the amyloid plaques found in Alzheimer disease (AD), which are predominantly composed of the 42-amino-acid-residue fragment, the vascular amyloid in CAA is mostly composed of the more soluble, 40-amino-acid fragment, which suggests different pathophysiological mechanisms for pathological deposition [1]. Impairment in one or more elimination mechanisms may result in the accumulation of Aβ in the walls of small- and medium-sized leptomeningeal and cortical blood vessels. Upon autopsy, CAA may be found more commonly in women than in men. The incidence of CAA, like AD, is strongly age-dependent. Although found at autopsy in only 33 % of 60–70 year olds, the prevalence of age-related CAA increases to 75 % among those older than 90 years [2]. Despite its high prevalence, CAA remains an underestimated cause of cerebrovascular disease, both clinically and at imaging, in part because many patients are asymptomatic. When symptomatic, intracerebral haemorrhage (ICH) in the elderly is the most well-known manifestation. Furthermore, the clinical presentation varies from a sudden neurological deficit to seizures, transient symptoms and cognitive decline, including acute progressive dementia. However, these symptoms are not specific and are often not readily associated with CAA.

Radiologically, in addition to typical acute cortical-subcortical ICH, CAA leads to various types of abnormal findings, including chronic ICHs, microbleed (MB), subarachnoid haemorrhage (SAH), superficial siderosis (SS), microinfarction, reversible oedema and irreversible leukoaraiosis (Table 1) [3]. Taking into consideration the clinical importance of CAA-related haemorrhagic risks in the setting of antiplatelet, anticoagulation and thrombolysis therapies, as well as treatable oedema [3–6], it is necessary for radiologists to understand the wide spectrum of CAA-related imaging findings.

The aims of this study were the following: to expound the characteristics of neuroimaging modalities, including computed tomography (CT), magnetic resonance imaging (MRI) and positron emission tomography (PET), which cover a wide spectrum of CAA-related imaging findings, and to review the various abnormal findings for which CAA could be responsible. The recognition of wide-spectrum imaging findings can be useful for radiologists not only to raise the possibility of CAA but also to precisely comprehend the pathophysiology of CAA and management to improve the prognosis.

Neuroimaging modalities: critical roles in the diagnosis of CAA

CT

CT is the initial screening modality for patients with various symptoms, especially acute neurological deficits or transient ischaemic attack-like symptoms, which can allow rapid establishment of the presence or absence of ICHs and SAHs. CT can provide crucial information regarding the characteristics of these haemorrhagic conditions, including volume, shape and distribution. Additional CT angiography with intravenous contrast media is useful to exclude other pathological conditions (e.g. aneurysms, arteriovenous malformation, fistula and venous thrombosis) that could cause similar haemorrhagic complications.

On CT scan, cortical-subcortical ICHs without a history of hypertension and sulcal SAHs without a history of head trauma can be the findings suggestive of CAA. However, it is difficult to evaluate other findings, such as MBs and SS, which support the diagnosis of CAA. The disadvantage of CT is lower contrast resolution than MRI, which can depict acute cerebral infarctions, MBs and white matter lesions more clearly. In other words, CAA cannot be diagnosed by CT alone, but requires MRI sequences sensitive to susceptibility effects.

MRI

The important point of MRI in the diagnosis of CAA is to perform the proper sequences to cover a wide spectrum of CAA-related abnormal findings including not only haemorrhages but also oedemas and infarctions. Therefore, the standard imaging protocol should include at least the gradient-echo (GRE), fluid-attenuated inversion recovery (FLAIR) and diffusion-weighted imaging (DWI). The standard MRI protocol is shown in Table 2.

The optimal detection of haemorrhagic lesions, including MB and SS, depends on multiple MRI parameters, including pulse sequence, spatial resolution, echo time and field strength. Due to CAA-related pathological changes such as haemosiderin accumulations which lead to large variations in local magnetic fields and a local reduction in T2*, it is necessary to perform the GRE sequence, which is more sensitive to the magnetic susceptibility effect than turbo spin-echo sequences, in the diagnosis of CAA [7]. In the elderly, GRE sequences are essential to check for CAA-related MBs and/or SAH, which can potentially predict life-threatening lobar haemorrhages [8]. Compared with conventional 2D sequences, increasing spatial resolution (i.e. smaller voxel size) on 3D sequence improves the detection of MBs [9]. A longer echo time enables more efficient detection of MBs than a shorter one due to the blooming effect [9]. In addition to these parameters, higher susceptibility effects and increase of

Table 1 CAA-related abnormal imaging findings

Disease	Imaging findings	Recommended neuroimaging modality
ICH	Haematoma with distinctive cortical-subcortical distribution generally sparing the deep white matter and basal ganglia and brainstem	CT and MRI **MRI**; additional depiction of chronic haemosiderin depositions and MBs
MBs	Small round hypointense foci on MRI	MRI, especially susceptibility-weighted image
SAH	Supratentorial sulcal high attenuation/intensity, most frequently depicted around the precentral gyrus	CT and MRI **MRI**; additional depiction of MB and SS
SS	Hypointensity along the supratentorial cerebral sulcus on MRI	MRI, especially susceptibility-weighted image
CAA-related inflammation	Large confluent asymmetric abnormal attenuation/intensity mainly in the subcortical WM	CT and MRI **MRI**; additional evaluation of vasogenic oedema and other findings such as MB and SS
Leukoaraiosis	Low attenuation on CT and high intensity on FLAIR and T2W MRI mainly in the deep WM with sparing of the subcortical U fibres	CT and MRI MRI; depiction of leukoaraiosis clearer than CT
Microinfarction	Small ovoid or round high intensity of the subcortical and cortex on diffusion-weighted image	MRI, especially diffusion-weighted image

CAA cerebral amyloid angiopathy, *CT* computed tomography, *FLAIR* fluid-attenuated inversion recovery, *ICH* intracerebral haemorrhage, *MRI* magnetic resonance imaging, *MB* microbleed, *SAH* subarachnoid haemorrhage, *SS* superficial siderosis, *T2W* T2-weighted, *WM* white matter

signal-to-noise ratio with field strength improve the detection of MBs at a 3-T imager compared with a 1.5-T one [9]. Taking these parameters into consideration, it is reasonable to perform sophisticated 3D sequences with higher spatial resolution and longer echo time including a susceptibility-weighted image (SWI) and the principles of echo-shifting with a train of observations (PRESTO) image to detect MB and SS [9, 10]. Notably, SWI with smaller section thickness and higher magnetic field is currently the most sensitive technique to visualise MBs, which combines both magnitude information and phase information to accentuate the visibility of susceptible foci. These sequences can be of potential value in the evaluation of CAA patients (Fig. 1).

However, the GRE sequence is less sensitive than the FLAIR sequence for the detection of acute SAHs and parenchymal changes. The better lesion/tissue contrast achieved by the suppression of the signal intensity of cerebrospinal fluid (CSF) on the FLAIR sequence not only in the subarachnoid space, but also in the cerebral parenchyma can be especially useful for the evaluation of CAA-related white matter lesions and SAHs. In addition to these sequences, DWI with apparent diffusion coefficient (ADC) maps can be useful to distinguish CAA-related silent infarctions from other white matter lesions, including vasogenic oedema and leukoaraiosis [3, 5].

PET

Although clinical criteria based on MRI and CT findings have been validated for a pre-mortem diagnosis of CAA during life [11], this relies on detecting late manifestations of CAA-related vascular damage such as ICHs and MBs rather than the vascular amyloid itself. Therefore, these morphological

Table 2 Standard MRI protocol for the diagnosis of CAA

Sequence	Expected role for the diagnosis
Minimum required protocol	
T2*-weighted image	Depiction of haemosiderin depositions suggestive of chronic ICHs, MBs and SS
Fluid-attenuated inversion recovery image	Depiction of acute and subacute SAHs, and white matter signal changes
Diffusion-weighted image	Depiction of acute microinfarction Evaluation of vasogenic oedema due to CAA-related inflammation
Optional sequence for the diagnosis of CAA	
Susceptibility-weighted image	Depiction of haemosiderin depositions, clearer than T2*-weighted image
Additional sequences for differential diagnosis	
T1-weighted image	Depiction of T1 shortening due to methaemoglobin and melanin
Contrast-enhanced T1-weighted image	Differentiation between haemorrhagic tumours and other lesions
Magnetic resonance angiogram	Evaluation of vascular disorders such as vasculitis

CAA cerebral amyloid angiopathy, *ICH* intracerebral haemorrhage, *MB* microbleed, *MRI* magnetic resonance imaging, *SAH* subarachnoid haemorrhage, *SS* superficial siderosis

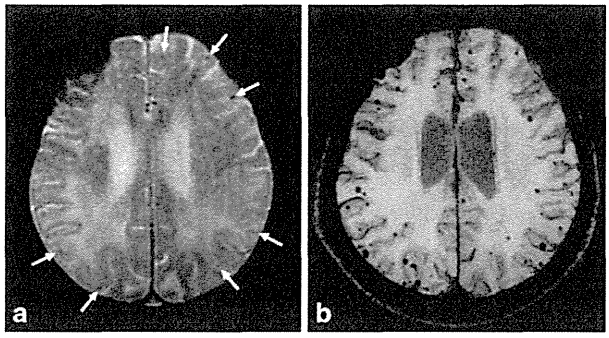

Fig. 1 Multiple MBs and CAA-related inflammation in a 78-year-old man. In addition to the right dominant diffuse white matter lesions, an axial GRE T2*-weighted image on the 1.5-T imager (**a**) revealed some cortical-subcortical hypointense foci suggestive of CAA-related MBs (*arrows*). Of note, more hypointense foci in the posterior dominant distribution were identified on the corresponding PRESTO image (**b**)

techniques cannot lead to a correct diagnosis in a definite proportion of CAA patients during life. However, an emerging functional technique, Pittsburgh compound B (PiB) PET imaging to measure the burden and location of fibrillar Aβ deposits, has recently been reported as a promising technique for CAA detection [12]. In addition to binding to fibrillar senile plaques, this radiotracer can clearly delineate the vascular amyloid before it triggers haemorrhagic complications or other overt small-vessel brain injuries, and can be a useful clue to diagnose not only AD but also CAA [13].

In the case of coexisting CAA and hypertension, the widespread involvement of arterioles by both types of arteriopathy likely causes the progression of small vessel disease and some overlap in the distribution of MBs [14]. In such cases, PiB-PET can provide a definite clue not only for the diagnosis of CAA but also the coexistence of hypertensive arteriopathy (Fig. 2). However, it is important to understand that PIB is a non-specific imaging marker of Aβ peptide-related cerebral amyloidosis. As previously mentioned, this tracer labels vascular as well as plaque Aβ; therefore, differentiating PiB signal caused by CAA from that caused by other kinds of plaques is difficult.

Representative imaging findings: multifaceted features of a single pathological condition

Lobar haemorrhage: a life-threatening sign

CAA is one of the most common causes of lobar ICHs in the elderly [15]. In addition to the advanced age, hypertension and minor head injuries may increase the risk of CAA-related ICHs [15, 16]. The clinical presentation of CAA-related ICH varies according to ICH size and location. Patients commonly present with an acute stroke syndrome with focal neurological deficits that may be associated with headache, vomiting, seizures and/or an altered level of consciousness. In the longer term, survivors of lobar ICHs are at a high risk of recurrence, especially with the presence of the ε2 or ε4 alleles of the apolipoprotein E gene (28 % cumulative recurrence rate at 2 years relative to 10 % in patients without either allele) [17].

Regardless of the size, CAA-related ICHs exhibit distinctive cortical-subcortical distributions that generally spare the deep white matter, basal ganglia and brainstem. This cortical-subcortical distribution of CAA-related ICHs has been correlated with the anatomical distribution of β-amyloid-containing vessels. Notably, haemorrhagic lesions are shown to be preferentially distributed in the temporal and occipital lobes, and are likely to cluster regardless of the lobes [18]. Comprehension of this characteristic distribution was validated by the Boston criteria, which are most commonly used and highly specific for the diagnosis of CAA (Table 3) [11, 19]. CAA-related macrohaemorrhages may be associated with subarachnoid, subdural or, less commonly, intraventricular haemorrhage (Figs. 3 and 4) [8]. Other neuroimaging findings suspicious for CAA-related ICHs include the multiplicity and recurrence of ICHs (Fig. 4). Recurrent haemorrhages are typically lobar, often in the same lobe as the initial CAA-related ICHs [18]. CT is sufficient to provide crucial information regarding the characteristics of acute CAA-related ICHs. However, MRI examinations including GRE sequences should be performed to evaluate chronic haemosiderin depositions and MBs, which can be useful to diagnose CAA.

Microbleeds: easily overlooked but a suggestive sign of CAA

This finding indicates previous extravasation of blood-related to bleeding-prone microangiopathy, including CAA and hypertensive arteriopathy (Fig. 5) [14]. In the pathological analysis of lobar MBs in CAA patients, various CAA-related pathologies, including acute microhaemorrhages, haemosiderin residua of old haemorrhages and small lacunes ringed by haemosiderin, are proved to produce signal voids on SWI [20]. MBs located in lobar regions may correlate with disease progression, recurrent ICH, and cognitive dysfunctions [21, 22]. Moreover, early recognition can be advantageous to patients on antiplatelet or thrombolysis therapy in that they are at an increased risk for subsequent and possibly fatal haemorrhages [4, 6].

MBs are typically defined on GRE sequences as small, well-demarcated, hypointense, rounded foci less than 5–10 mm in size, which are distinct from cortical vascular flow voids, leptomeningeal siderosis, or non-haemorrhagic subcortical mineralisation such as symmetrical hypointensities in the globus pallidus [21]. The presence of multiple, strictly lobar, cortical-subcortical MBs detected by GRE sequences has been shown to be highly specific for severe CAA in elderly patients with no other definite cause of ICH, such as trauma, ischaemic stroke, coagulopathy or excessive anticoagulation (probable

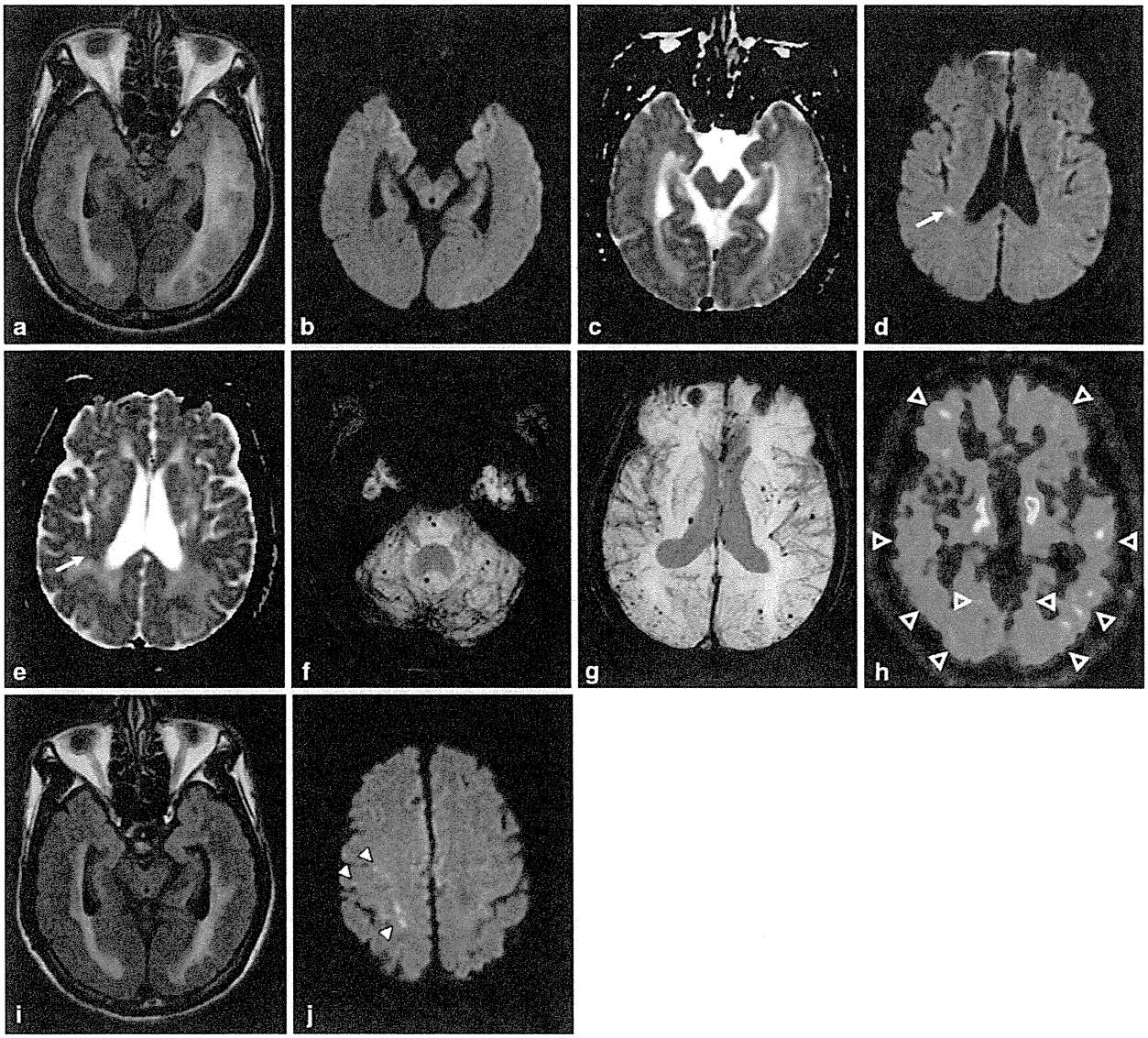

Fig. 2 CAA-related inflammation, MBs, and microinfarctions in a 72-year-old man. An axial FLAIR image (**a**) showed large confluent asymmetric hyperintense lesions, which involved not only the left dominant subcortical white matter but also the overlying left temporo-occipital cortices, with a mass effect. Low signal intensity on DWI (**b**) and increased diffusion on the ADC map (**c**) suggested vasogenic oedema. In addition to these white matter lesions, DWI (**d**) demonstrated a small right temporal hyperintense lesion (*arrow*) with corresponding decreased diffusion (*arrow*) on the ADC map (**e**) (*arrow*). This signal change indicated a relatively acute microinfarction. An axial 3D T2*-weighted image (**f**, **g**) revealed multiple MBs, which were distributed not only in the posterior dominant cortical-subcortical region but also in the left putamen, right thalamus, pons and cerebellum. A PiB-PET image (**h**) revealed the diffuse cortical accumulation, including the occipital lobes, higher than those of the cerebral white matter, which indicated the global PiB uptake (*open arrowheads*). These finding of MBs and PiB distribution suggested the coexistence of CAA and hypertensive arteriopathy. Two months after a course of intravenous steroid therapy, an improvement in the white matter lesions was identified on a FLAIR image (**i**). However, DWI (**j**) revealed new subcortical microinfarctions in the right frontal lobe (*arrowheads*)

CAA on the Boston criteria in the Table 3) [11]. Similar to the distribution of CAA pathology and CAA-related lobar ICHs, the distribution of CAA-related MBs appears to show a posterior cortical predominance (Figs. 1, 2 and 6) [18]. GRE sequences are the recommended method for MB detection due to the insensitivity of MB detection on CT and spin-echo sequences of MRI. Furthermore, considering the limitation of conventional T2* GRE sequences, which have underestimated MBs in 25 % of CAA patients, more sensitive sequences such as SWI and PRESTO sequences should be used to increase the detection rates of MBs (Fig. 1) [9]. It is notable that neuroimaging study has revealed lobar MBs in more than 20 % of patients with AD (Fig. 7), which may reflect advanced CAA in keeping with neuropathological findings [23].

Table 3 Classic and modified Boston criteria [11, 19]

	Classic Boston criteria	Modified Boston criteria
Definite CAA	Full post-mortem examination demonstrating: - Lobar, cortical or corticosubcortical haemorrhage - Severe CAA with vasculopathy - Absence of other diagnostic lesion	No modification
Probable CAA with supporting pathology	Clinical data and pathological tissue (evaluated) haematoma or cortical biopsy) demonstrating: - Lobar, cortical or corticosubcortical haemorrhage - Some degree of CAA in specimen - Absence of other diagnostic lesion	No modification
Probable CAA	Clinical data and MRI or CT demonstrating: - Multiple haemorrhages restricted to lobar, cortical or corticosubcortical regions (cerebellar haemorrhage allowed) - Age ≥55 - Absence of other cause of haemorrhage	Clinical data and MRI or CT demonstrating: - Multiple haemorrhages restricted to lobar, cortical or corticosubcortical regions (cerebellar haemorrhage allowed), or - Single lobar, cortical, or corticosubcortical haemorrhage and focal or disseminated superficial siderosis - Age ≥55 - Absence of other cause of haemorrhage or superficial siderosis
Possible CAA	Clinical data and MRI or CT demonstrating: - Single lobar, cortical or corticosubcortical haemorrhage - Age ≥55 - Absence of other cause of haemorrhage	Clinical data and MRI or CT demonstrating: - Single lobar, cortical or corticosubcortical haemorrhage, or - Focal or disseminated superficial siderosis - Age ≥55 - Absence of other cause of haemorrhage or superficial siderosis

Subarachnoid haemorrhage: a predictive finding of unfavourable outcomes?

Recently, CAA has been increasingly reported as a cause of SAHs in the elderly, especially those localised at the convexity of the brain (cSAH) [24, 25]. CAA-related cSAH may be due to direct extension of the cortical-subcortical haemorrhage into the subarachnoid or to primary SAH resulting from disruption of the leptomeningeal vessels by β-amyloid (Figs. 4 and 6) [8]. The clinical presentation of CAA-related cSAH is distinct because patients suffer from transient focal neurological deficits, including motor or sensory symptoms and seizures, rather than typical headaches [24, 25]. Such symptomatic cSAHs are mainly located within the central sulcus. Whether cSAH could be a warning sign of subsequent ICHs depends on the underlying disease. CAA-related cSAH often recurs, and a high rate of subsequent cerebrovascular disorders including infarctions and ICHs could contribute to unfavourable outcomes, including neurological disability and death in the elderly [25, 26].

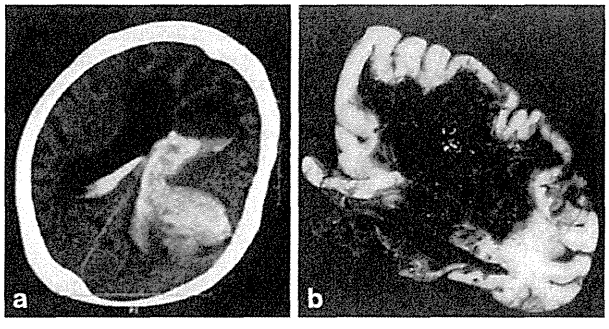

Fig. 3 Fetal CAA-related ICH with associated massive ventricular haemorrhage in a 92-year-old woman. A CT scan (**a**) revealed large left-sided parietal subcortical ICH extending into the left lateral ventricle, which caused hydrocephalic ventricular dilatation. A huge subcortical and intraventricular haematoma was identified on a macroscopic specimen at autopsy (**b**)

Unenhanced head CT has shown a slight, sometimes barely visible, sulcal hyperattenuation, most frequently depicted around the precentral gyrus [26]. Subsequent MRI scans confirmed the subarachnoid haemorrhage as a hyperintense area on FLAIR images (Fig. 6). In addition to this subarachnoid lesion, GRE sequences, especially SWI and PRESTO images, showed multiple lobar cortical-subcortical haemorrhagic lesions (macrohaemorrhages or MBs) (Fig. 6) [24, 25]. Considering the high prevalence of MBs and SS in CAA patients [24], these abnormal findings should be evaluated in the diagnosis of cSAH. It is also to be noted that CAA-related cSAH and SS can be present without other haemorrhagic lesions, including ICHs and MBs [19].

Superficial siderosis: a clinical entity distinct from the well-known classical SS

It is estimated that repeated cSAH leads to haemosiderin deposits in the subpial layers of the supratentorial brain [19].

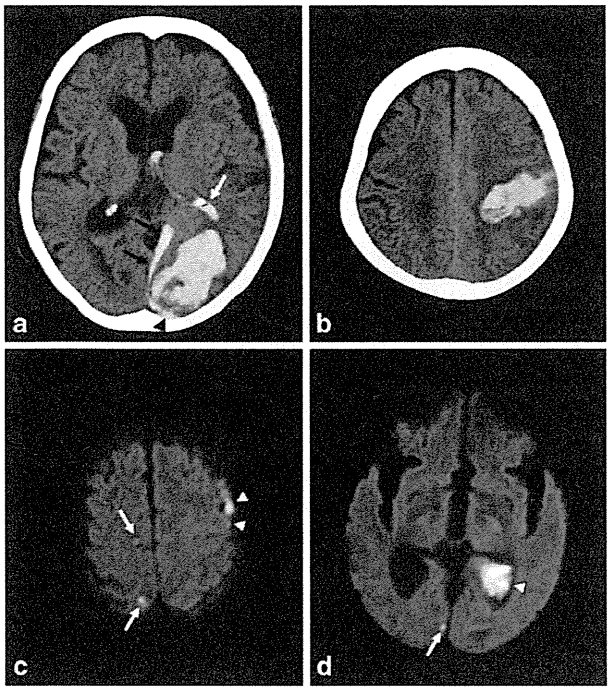

Fig. 4 Recurrent CAA-related ICHs associated with intraventricular, subdural and subarachnoid haemorrhages, and microinfarctions in an 87-year-old woman. A CT scan (**a**) showed left-sided occipital subcortical ICH extending into the left lateral ventricle (*white arrow*), and the subdural (*black arrows*) and subarachnoid space (*arrowhead*) around the occipital lobe. Seven months later, left-sided parietal subcortical ICH recurred and extended into the left ventricle. In addition to these haemorrhagic lesions, asymptomatic cortical microinfarctions (*arrows*) were identified on DWI 12 days after the first (**c**) and 13 days after recurrent ICH (**d**). *Arrowheads* indicated subdural, subarachnoid and intraventricular haemorrhages

In addition to other lobar haemorrhagic lesions, SS depicted predominantly in the supratentorial area has been increasingly recognised as one of the CAA-related abnormal findings [24]. A recent report has revealed that CAA-related SS as well as cSAH can be a warning sign of future intracranial haemorrhagic lesions [27].

Considering the marked difference of SS prevalence observed between CAA and non-CAA patients, the inclusion of SS in the modified Boston criteria may enhance their sensitivity for the diagnosis of CAA without a loss in specificity (Table 3) [19]. Furthermore, SS can be the important indicator of CAA in AD patients beyond the MBs or ICHs that are more readily recognised as being CAA-related haemorrhagic lesions (Fig. 7) [28].

CAA-related SS on GRE sequences showed the characteristic 'gyriform' pattern of a hypointense signal (Figs. 6 and 7). Generally, proton density and FLAIR images or unenhanced CT scans are used to identify acute SAHs and to distinguish them from chronic SS [27]. This abnormal signal intensity revealed a preference for the cerebral convexity and only exceptionally occurred in the infratentorial area [19]. This distribution explains why CAA-related SS may be associated with transient neurological manifestations and lacks the typical clinical presentation associated with the well-known SS, namely cerebellar and brainstem signs [19].

CAA-related inflammation—treatable form of a CAA-related disorder

In addition to haemorrhagic complications, a syndrome of perivascular inflammation and oedema has been recognised in the spectrum of presentations associated with CAA [29]. Pathologically, CAA-related inflammation reveals vascular amyloid deposition accompanied by perivascular, intramural and/or transmural inflammatory changes, with or without granuloma formation. The mechanism by which this immune response occurs is not well understood, although one possible factor is the increased frequency of the apolipoprotein E ε4/ε4 genotype [5, 29]. The clinical presentation of CAA-related inflammation typically manifests as headache, subacute cognitive decline and seizures [5, 29]. The apparent response of most patients to immunosuppressive therapy suggests that this disorder represents a treatable form of CAA, which highlights the importance of reaching this diagnosis in practice (Fig. 2).

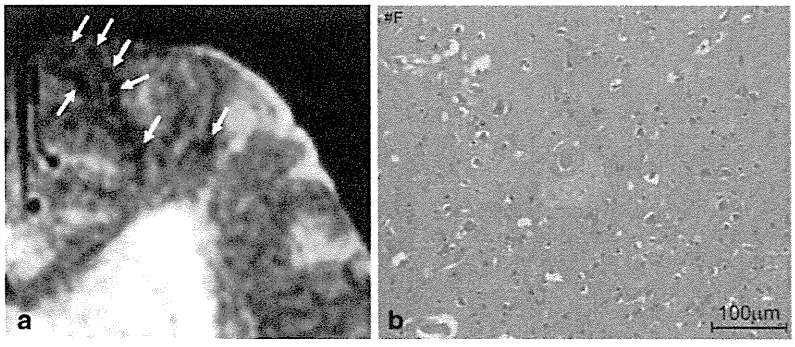

Fig. 5 Pathologically proved subcortical MBs in a 76-year-old man. An axial GRE T2*-weighted image (**a**) showed multiple cortical-subcortical hypointense foci suggestive of CAA-related MBs (*arrows*). A histopathological section corresponding to MBs (haematoxylin and eosin stain) (**b**) revealed amyloid deposits in the vessel walls with perivascular leakage of erythrocytes and plasma

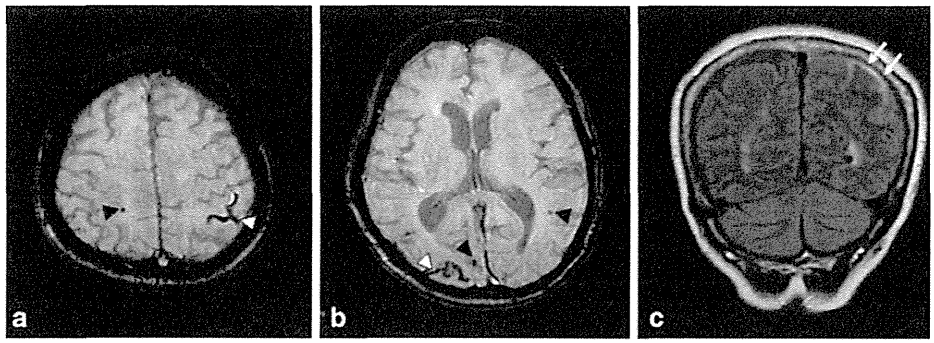

Fig. 6 Non-traumatic SAH at the convexity of the brain, microbleed and SS in a 72-year-old woman who was clinically diagnosed with AD. Axial 3D T2*-weighted images (**a**, **b**) showed bilateral subcortical MBs (*black arrowheads*) and sulcal SS (*white arrowheads*) in the posterior dominant distribution. Additionally, SAH along the left parietal sulci (*arrows*) was identified on a coronal FLAIR image (**c**)

However, CAA-related inflammation could also be not only a stable/progressive disorder but also a relapsing disorder, and the proportion crossing over from "improved" to "relapsing" disease may increase with longer follow-ups [5].

CAA-related inflammation is characterised by large confluent asymmetric white matter lesions of abnormal attenuation/intensity extending to the subcortical white matter and occasionally the overlying cortical grey matter with mass effect (Figs. 1 and 2). These lesions are depicted more clearly on MRI than on CT, especially on the FLAIR sequence, and involve one or more cortical territories, distributed almost equally across the frontal, parietal, temporal and occipital

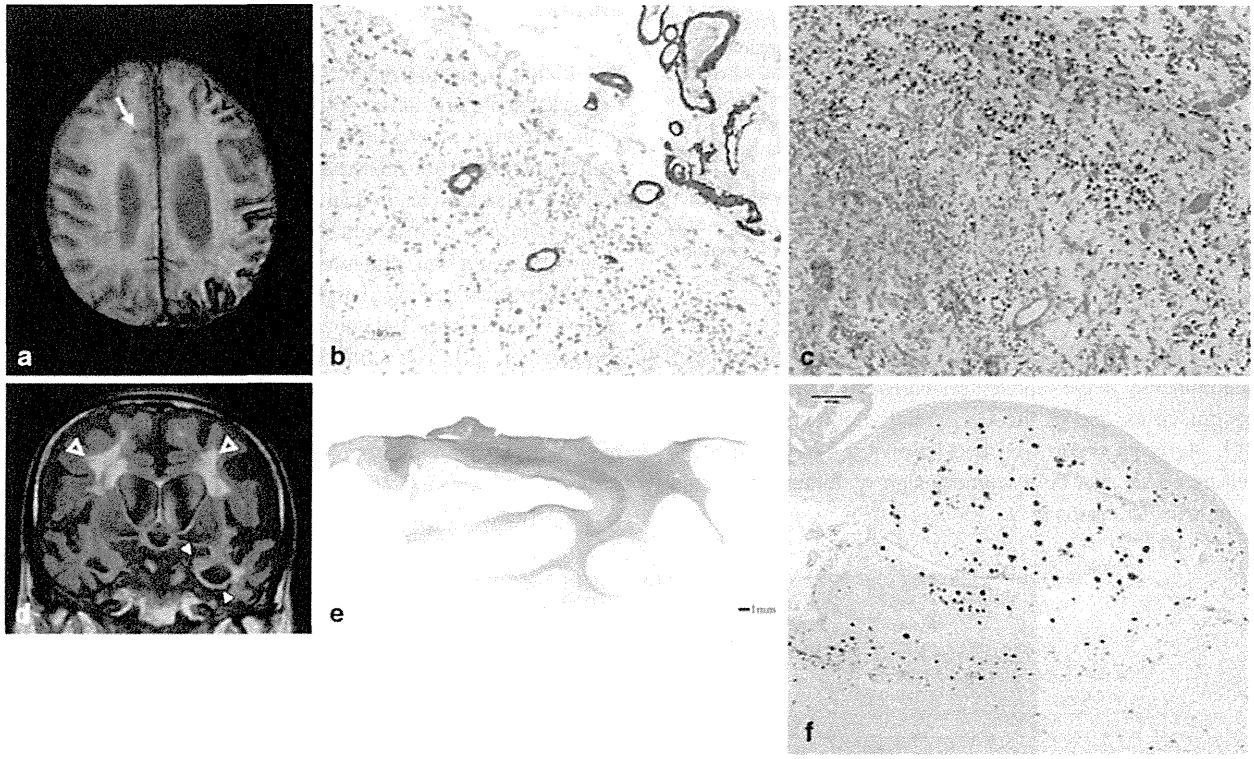

Fig. 7 CAA-related SS and MB in a 90-year-old man with pathologically proved AD. In addition to the right frontal subcortical MB (*arrow*), a 3D T2*-weighted image (**a**) demonstrated the typical gyriform low signals along the left cerebral sulci. Severe amyloid beta immunoreactive deposits were present in the leptomeningeal and cortical vessel walls of the parietal lobe (immunohistochemistry raised against monoclonal antibody Aβ 11–28) (**b**). The upper cortical layers were necrotic. Numerous haemosiderin-laden macrophages were present in the subarachnoid space and upper cortical layers (haematoxylin and eosin stain). These findings were consistent with superficial siderosis. A coronal FLAIR image (**d**) demonstrated left dominant atrophy of the amygdala and parahippocampal gyrus (*arrowheads*), and symmetric deep white matter hyperintensities (*open arrowheads*). A section of the left posterior hippocampus revealed atrophy of the hippocampus proper, subiculum and parahippocampal gyrus. Pallor of the subcortical white matter was evident (Klüver-Barrera stain) (**e**). There were numerous Aβ 11–28 immunoreactive senile plaques in the hippocampus (**f**)

lobes without evident preferential laterality [5]. DWI and ADC maps can add further information suggestive of vasogenic oedema (Fig. 2). Interestingly, the clinical and neuroimaging feature of this condition is similar to the vasogenic oedema of amyloid-related imaging abnormalities (ARIA) associated with amyloid-modifying therapy. A potential connection between CAA-related inflammation and immunotherapy-associated ARIA has been recently suggested by identification of anti-Aβ autoantibodies in the CSF of a patient with the spontaneously occurring syndrome [30].

Leukoaraiosis: a common but by no means specific finding of CAA

Leukoaraiosis is a radiological term which describes the abnormal imaging changes in the deep cerebral white matter. Pathological changes include demyelination, axon loss and mild gliosis. CAA-related impairments of perfusion due to amyloid in the overlying cortical small vessels probably cause the leukoaraiosis in CAA patients [3, 32]. Another possible mechanism of leukoaraiosis in CAA is as a result of the accumulation of silent ischaemic lesions [3].

Leukoaraiosis appears as diffuse or focal low attenuation on CT or hyperintensity on T2-weighted and FLAIR images on MRI, which is prevalent in the centrum semiovale and deep white matter with sparing of the subcortical U fibres (Figs. 7 and 8) [8]. In contrast to CAA-related inflammation, this finding is irreversible. As well as hypertensive arteriopathy, CAA-related leukoaraiosis preferentially affects the same periventricular regions; however, some studies suggest the posterior dominant white matter involvement in CAA patients [3, 32] (Fig. 8). Although advanced CAA is associated with a large burden of white matter lesions compared with healthy elders and AD patients, these lesions are basically non-specific and not useful for the diagnosis of CAA.

Microinfarction: a clinically silent event suggestive of progressive arteriopathy

Recent studies using MR DWI, which is very sensitive to even small ischaemic lesions, have demonstrated that acute and subacute ischaemic infarctions are not infrequent in patients with advanced CAA, and occur in approximately 15 % of these patients [31, 32]. Analyses of autopsied brains with advanced CAA have identified lesions described as perivascular scars or small infarctions at frequencies ranging from 37 % to nearly 100 % [32]. These pathologically observed infarctions are frequently multiple and located in the cortical ribbon or underlying subcortical white matter. Impaired cerebral blood flow regulation due to CAA-related occlusive arteriopathy may be related to these ischaemic changes [32]. Their presence was shown to be unrelated to conventional vascular risk factors such as hypertension, diabetes and coronary artery disease, and was instead associated with the severity of white matter lesions and lobar MBs, which suggests that they are due to CAA-related occlusive arteriopathy [31]. These lesions appear to be clinically asymptomatic; however, the therapeutic implications and prognostic significance of these findings require further study.

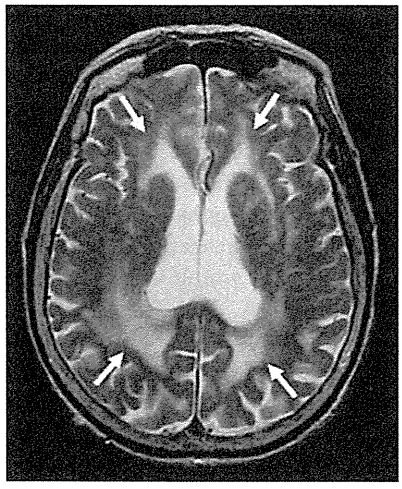

Fig. 8 Leukoaraiosis in an 87-year-old woman with pathologically proved CAA and AD. Axial T2-weighted images showed bilateral hyperintensities (*arrows*), which involved the posterior dominant periventricular and deep white matters

On MRI, these lesions are located mainly in the subcortical white matter and cortical grey matter away from the site of previous ICHs [31, 32]. They may also be located in the cerebellum. Acute lesions were identified as small and mostly ovoid or round bright areas on DWI sequences and corresponding dark areas on ADC maps (Figs. 2 and 4).

CAA and AD—representation of two sides of a single condition: Aβ amyloidosis

Pathologically, CAA is commonly found in AD (Fig. 7), with a prevalence of more than 80 % [2]. The high prevalence of CAA in patients with AD as well as of cerebral parenchymal Aβ deposition (senile plaques) in patients with CAA can be explained by AD and CAA representing two sides of a single condition. Therefore, the degree of CAA in AD is more severe than that in non-AD patients. It is noteworthy that the presence of CAA may have a significant impact on the clinical course of AD. The coexistence of CAA with AD has been reported to impair cognitive performance more significantly than AD alone, even after adjustments for age, neurofibrillary tangle and amyloid plaque number, and infarctions [33].

Differential diagnosis

A single large cortical-subcortical ICH presenting with an acute neurological deficit is not entirely specific for a

diagnosis of CAA. Various disorders, including hypertensive arteriopathy, haemorrhagic tumours, vascular malformation, trauma, bleeding diatheses and illicit drug use such as amphetamines and cocaine, can cause cortical-subcortical ICHs [8]. Notably, infectious aneurysm can cause not only subcortical ICH but also SAH and MBs like signal change. In the diagnosis of subcortical haemorrhagic lesions, it is sometimes difficult to narrow the differential diagnosis because of its non-specific nature. Therefore, to evaluate other abnormal findings suggestive of CAA (i.e. MBs and SS) is mandatory for the precise diagnosis. Gadolinium enhancement and MR angiogram are also useful to evaluate the tumorous and vascular lesions, respectively.

The hypertensive arteriopathy as well as CAA is the most common cause of MBs. Less common causes include diffuse axonal injury, cerebral fat embolism, cerebral autosomal dominant arteriopathy with subcortical infarcts and leukoencephalopathy (CADASIL), multiple cavernous malformations, vasculitis, radiation vasculopathy and so on. To understand the distinctive cortical-subcortical distributions that generally spare the basal ganglia and brainstem is important for the diagnosis of CAA. To check the other imaging findings such as restricted diffusion of axonal injury, multiple white matter lesions—especially in the temporal pole of CADASIL—and vascular lesions of vasculitis, are also contributory to diagnosis.

Convexal SAH and SS are important subtypes of nonaneurysmal subarachnoid bleeding and its sequela with diverse aetiologies. Although CAA is frequent in patients older than 60 years, a reversible vasoconstriction syndrome appears to be a common cause of cSAH in younger patients [24]. Other than those above, cSAH carries a broad differential diagnosis, including head trauma, posterior reversible encephalopathy syndrome (PRES), dural sinus and cortical venous thrombosis, vascular malformation, vasculitis and anticoagulation [34]. Parenchymal abnormalities, including cerebral contusions and subcortical white matter lesions, are useful to diagnose head trauma and PRES. Additionally, to check the vascular lesion, especially the dural sinus and cortical vein, is crucial for the diagnosis of thromboses and malformations.

Because various pathological conditions, including PRES, infections (e.g. progressive multifocal leukoencephalopathy), acute disseminated encephalomyelitis and malignancies (e.g. primary CNS lymphoma and gliomatosis cerebri), can manifest as multiple white matter lesions [35], the essential step in the diagnosis of CAA-related inflammation is the recognition of CAA. In other words, GRE sequences including SWI and PRESTO images, which enable recognition of CAA-related MBs and SS, are fundamental in diagnosing CAA-related inflammation without invasive brain biopsy (Fig. 2) [5]. Considering that a part of the CAA-related inflammation may manifest as non-haemorrhagic white matter lesions, PiB-PET should be regarded as a supplementary diagnostic technique.

In addition to above-described imaging findings, it is also necessary to evaluate the medical history, physical examination findings and laboratory results to differentiate CAA from its mimickers. For example, typical medical history such as the elevated blood pressure and chemotherapy is usually associated with PRES and helps to clarify the diagnosis.

Conclusions

In the various types of CAA-related abnormal findings, haemorrhagic lesions, especially lobar restricted ICHs and MBs, cSAH and supratentorial SS, in the elderly can be crucial imaging findings of CAA. Furthermore, CAA can reveal other imaging findings including CAA-related inflammation and microinfarction. Radiologists should understand that MRI, especially GRE and FLAIR sequences, can non-invasively provide clues for the diagnosis of CAA-related disorders. CAA-related imaging findings are not always specific; therefore, it is necessary to combine with other CAA-related imaging findings for the diagnosis. Amyloid PET can be an important clue to differentiate CAA from other pathological conditions, such as hypertension and bleeding diatheses, which cause similar and mistakable haemorrhagic imaging findings.

Acknowledgments We have received the support for the English proofreading from a Grant-in-Aid for Scientific Research (Kakenhi C) (24591785, K.S. and 23500435, M.T.), Research on Measures for Intractable Diseases (M.T.) (H24-nanchi-ippan-063, Nanchi-ippan-013) and the Comprehensive Brain Science Network (S.M., M.T.).

References

1. Attems J, Lintner F, Jellinger KA (2004) Amyloid beta peptide 1–42 highly correlates with capillary cerebral amyloid angiopathy and Alzheimer disease pathology. Acta Neuropathol 107:283–291
2. Yamada M, Tsukagoshi H, Otomo E, Hayakawa M (1987) Cerebral amyloid angiopathy in the aged. J Neurol 234:371–376
3. Charidimou A, Gang Q, Werring DJ (2012) Sporadic cerebral amyloid angiopathy revisited: recent insights into pathophysiology and clinical spectrum. J Neurol Neurosurg Psychiatry 83:124–137
4. Biffi A, Halpin A, Towfighi A, Gilson A, Busl K, Rost N, Smith EE, Greenberg MS, Rosand J, Viswanathan A (2010) Aspirin and recurrent intracerebral hemorrhage in cerebral amyloid angiopathy. Neurology 75:693–698
5. Kinnecom C, Lev MH, Wendell L, Smith EE, Rosand J, Frosch MP, Greenberg SM (2007) Course of cerebral amyloid angiopathy-related inflammation. Neurology 68:1411–1416
6. McCarron MO, Nicoll JA (2004) Cerebral amyloid angiopathy and thrombolysis-related intracerebral haemorrhage. Lancet Neurol 3: 484–492

7. Greenberg SM, Finklestein SP, Schaefer PW (1996) Petechial hemorrhages accompanying lobar hemorrhage: detection by gradient-echo MRI. Neurology 46:1751–1754
8. Chao CP, Kotsenas AL, Broderick DF (2006) Cerebral amyloid angiopathy: CT and MR imaging findings. Radiographics 26:1517–1531
9. Charidimou A, Krishnan A, Werring DJ, Rolf Jäger H (2013) Cerebral microbleeds: a guide to detection and clinical relevance in different disease settings. Neuroradiology 55:655–674
10. Sakurai K, Kawaguchi T, Kawai T, Ogino H, Hara M, Okita K, Yamawaki T, Shibamoto Y (2010) Usefulness of 3D-PRESTO imaging in evaluating putaminal abnormality in parkinsonian variant of multiple system atrophy. Neuroradiology 52:809–814
11. Knudsen KA, Rosand J, Karluk D, Greenberg SM (2001) Clinical diagnosis of cerebral amyloid angiopathy: validation of the Boston criteria. Neurology 56:537–539
12. Klunk WE, Engler H, Nordberg A, Wang Y, Blomqvist G, Holt DP, Bergström M, Savitcheva I, Huang GF, Estrada S, Ausén B, Debnath ML, Barletta J, Price JC, Sandell J, Lopresti BJ, Wall A, Koivisto P, Antoni G, Mathis CA, Långström B (2004) Imaging brain amyloid in Alzheimer's disease with Pittsburgh Compound-B. Ann Neurol 55:306–319
13. Greenberg SM, Grabowski T, Gurol ME, Skehan ME, Nandigam RN, Becker JA, Garcia-Alloza M, Prada C, Frosch MP, Rosand J, Viswanathan A, Smith EE, Johnson KA (2008) Detection of isolated cerebrovascular beta-amyloid with Pittsburgh compound B. Ann Neurol 64:587–591
14. Fazekas F, Kleinert R, Roob G, Kleinert G, Kapeller P, Schmidt R, Hartung HP (1999) Histopathologic analysis of foci of signal loss on gradient-echo T2*-weighted MR images in patients with spontaneous intracerebral hemorrhage: evidence of microangiopathy-related microbleeds. AJNR Am J Neuroradiol 20:637–642
15. Vinters HV (1987) Cerebral amyloid angiopathy. A critical review. Stroke 18:311–324
16. Arima H, Tzourio C, Anderson C, Woodward M, Bousser MG, MacMahon S, Neal B, Chalmers J, PROGRESS Collaborative Group (2010) Effects of perindopril-based lowering of blood pressure on intracerebral hemorrhage related to amyloid angiopathy: the PROGRESS trial. Stroke 41:394–396
17. O'Donnell HC, Rosand J, Knudsen KA, Furie KL, Segal AZ, Chiu RI, Ikeda D, Greenberg SM (2000) Apolipoprotein E genotype and the risk of recurrent lobar intracerebral hemorrhage. N Engl J Med 342:240–245
18. Rosand J, Muzikansky A, Kumar A, Wisco JJ, Smith EE, Betensky RA, Greenberg SM (2005) Spatial clustering of hemorrhages in probable cerebral amyloid angiopathy. Ann Neurol 58:459–462
19. Linn J, Halpin A, Demaerel P, Ruhland J, Giese AD, Dichgans M, van Buchem MA, Bruckmann H, Greenberg SM (2010) Prevalence of superficial siderosis in patients with cerebral amyloid angiopathy. Neurology 74:1346–1350
20. Schrag M, McAuley G, Pomakian J, Jiffry A, Tung S, Mueller C, Vinters HV, Haacke EM, Holshouser B, Kido D, Kirsch WM (2010) Correlation of hypointensities in susceptibility-weighted images to tissue histology in dementia patients with cerebral amyloid angiopathy: a postmortem MRI study. Acta Neuropathol 119:291–302
21. Werring DJ, Frazer DW, Coward LJ, Losseff NA, Watt H, Cipolotti L, Brown MM, Jäger HR (2004) Cognitive dysfunction in patients with cerebral microbleeds on T2*-weighted gradient-echo MRI. Brain 127:2265–2275
22. Greenberg SM, Eng JA, Ning M, Smith EE, Rosand J (2004) Hemorrhage burden predicts recurrent intracerebral hemorrhage after lobar hemorrhage. Stroke 35:1415–1420
23. Cordonnier C, van der Flier WM (2011) Brain microbleeds and Alzheimer's disease: innocent observation or key player? Brain 134:335–344
24. Kumar S, Goddeau RP Jr, Selim MH, Thomas A, Schlaug G, Alhazzani A, Searls DE, Caplan LR (2010) Atraumatic convexal subarachnoid hemorrhage: clinical presentation, imaging patterns, and etiologies. Neurology 74:893–899
25. Beitzke M, Gattringer T, Enzinger C, Wagner G, Niederkorn K, Fazekas F (2011) Clinical presentation, etiology, and long-term prognosis in patients with nontraumatic convexal subarachnoid hemorrhage. Stroke 42:3055–3060
26. Raposo N, Viguier A, Cuvinciuc V, Calviere L, Cognard C, Bonneville F, Larrue V (2011) Cortical subarachnoid haemorrhage in the elderly: a recurrent event probably related to cerebral amyloid angiopathy. Eur J Neurol 18:597–603
27. Linn J, Wollenweber FA, Lummel N, Bochmann K, Pfefferkorn T, Gschwendtner A, Bruckmann H, Dichgans M, Opherk C (2013) Superficial siderosis is a warning sign for future intracranial hemorrhage. J Neurol 260:176–181
28. Feldman HH, Maia LF, Mackenzie IR, Forster BB, Martzke J, Woolfenden A (2008) Superficial siderosis: a potential diagnostic marker of cerebral amyloid angiopathy in Alzheimer disease. Stroke 39:2894–2897
29. Eng JA, Frosch MP, Choi K, Rebeck GW, Greenberg SM (2004) Clinical manifestations of cerebral amyloid angiopathy-related inflammation. Ann Neurol 55:250–256
30. DiFrancesco JC, Brioschi M, Brighina L, Ruffmann C, Saracchi E, Costantino G, Galimberti G, Conti E, Curtò NA, Marzorati L, Remida P, Tagliavini F, Savoiardo M, Ferrarese C (2011) Anti-Aβ autoantibodies in the CSF of a patient with CAA-related inflammation: a case report. Neurology 76:842–844
31. Kimberly WT, Gilson A, Rost NS, Rosand J, Viswanathan A, Smith EE, Greenberg SM (2009) Silent ischemic infarcts are associated with hemorrhage burden in cerebral amyloid angiopathy. Neurology 72:1230–1235
32. Viswanathan A, Greenberg SM (2011) Cerebral amyloid angiopathy in the elderly. Ann Neurol 70:871–880
33. Pfeifer LA, White LR, Ross GW, Petrovitch H, Launer LJ (2002) Cerebral amyloid angiopathy and cognitive function: the HAAS autopsy study. Neurology 58:1629–1634
34. Spitzer C, Mull M, Rohde V, Kosinski CM (2005) Non-traumatic cortical subarachnoid haemorrhage: diagnostic work-up and aetiological background. Neuroradiology 47:525–531
35. Chung KK, Anderson NE, Hutchinson D, Synek B, Barber PA (2011) Cerebral amyloid angiopathy related inflammation: three case reports and a review. J Neurol Neurosurg Psychiatry 82:20–26

基礎講座　老年精神医学とBrain Imaging

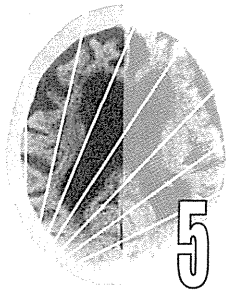

アミロイドイメージングの基礎

石井賢二（東京都健康長寿医療センター研究所神経画像研究チーム）

老年精神医学雑誌 24：503-512，2013

はじめに

アミロイドイメージングは生体におけるアミロイドβ（amyloid β；Aβ）の脳内沈着を非侵襲的に画像化できる診断技術であり，この技術の実用化が，アルツハイマー病（Alzheimer's disease；AD）の臨床研究にブレークスルーをもたらした．これは，従来は死後脳の病理学的検索から類推されていたAβ脳内沈着とAD発症との関係が，生きた人の経時的観察によって検証できるようになったからである．アミロイドカスケード仮説[11]では，Aβ脳内沈着がADの最も早期のイベントとして無症候のうちに始まり，それに引き続く神経機能障害，タウ沈着，神経細胞脱落，それらの総和的結果としての認知機能障害の発現，という病態進展の流れが想定されている．現在Alzheimer's Disease Neuroimaging Initiative（ADNI）研究をはじめとする追跡研究によって細部の病態メカニズムを確認しながら，疾患の早期診断・発症予測法を確立するとともに，どのようなタイミングで，どのような介入を行うことがこの疾患の克服につながるのかが検討されつつある．

アミロイドイメージングが脳における老人斑の密度を推定する診断技術であるならば，その有用性は臨床診断や他の画像診断との対比ではなく，死後ないし生検脳病理所見とPET所見とを対比することによってしか検証することはできない．

Kenji Ishii
〒173-0015　東京都板橋区栄町35-2

世界的標準薬として使われている^{11}C-PiB（Pittsburgh Compound-B）や，現在治験の進められている診断薬では，AD診断に匹敵するレベルの老人斑密度では，PETと病理の相関がきわめて良好にあることが確認されつつあり[12]，アミロイドイメージングを用いた臨床研究の意義もよりいっそう明確なものとなってきている．

2011年に27年ぶりに改訂されたADの臨床診断基準には，病態進展を客観的に示す指標として，アミロイドイメージングを含むバイオマーカーが組み込まれた（図1）[30]．こうした流れを背景に，2012年4月，アメリカ食品医薬品局（FDA）はアミロイドイメージング診断薬^{18}F-florbetapir（AV-45）を新薬として承認し，日常臨床での使用も可能となった．本稿では，アミロイドイメージングについて，これまでの知見を概説するとともに，今後のAD診療や治療薬開発になにをもたらすのかについて考察したい．

Ⅰ．アミロイドイメージング診断薬開発の現状

これまで提案されたアミロイドイメージング診断薬は，アミロイド組織染色に用いられている色素であるコンゴーレッドやチオフラビンTの類似化合物を放射性同位元素で標識したものである（図2）．ピッツバーグ大学のKlunkとMathisにより開発された^{11}C-PiBはAβに対する結合性の感度と特異性いずれもが高い優れた性質をもち，世界の多数の施設でこれを用いた臨床研究が積み

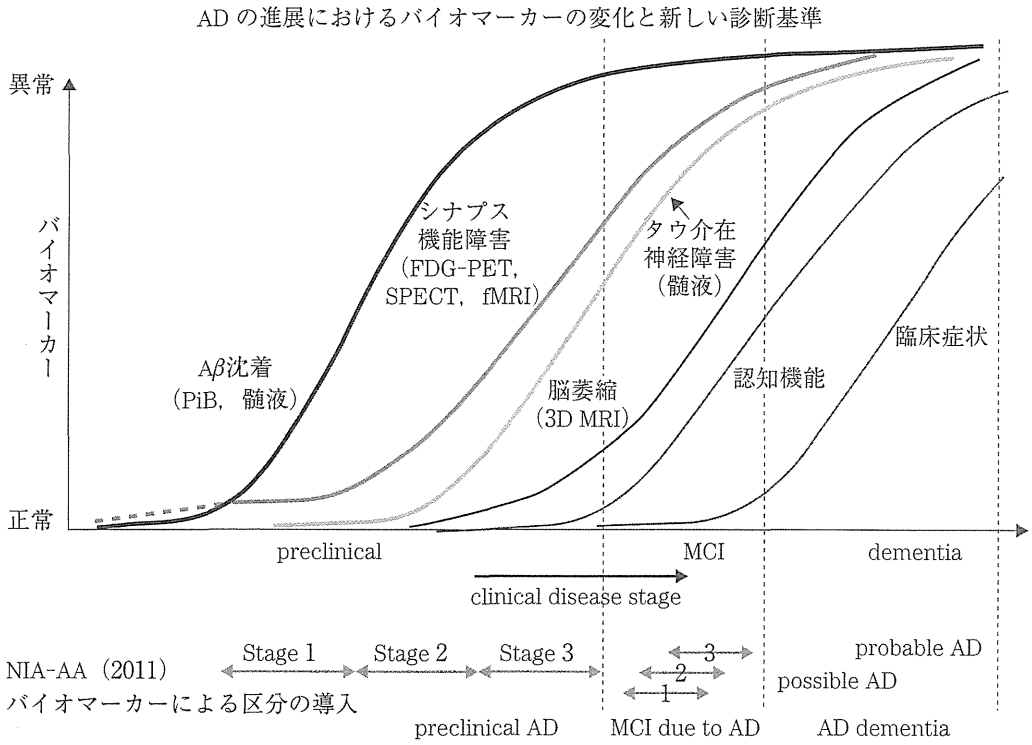

(Sperling RA, Aisen PS, Beckett LA, Bennett DA, et al.: Toward defining the preclinical stages of Alzheimer's disease ; Recommendations from the National Institute on Aging-Alzheimer's Association workgroups on diagnostic guidelines for Alzheimer's disease. *Alzheimers Dement*, 7 : 280-292, 2011 より改変引用)

図1　新しいアルツハイマー病診断基準（NIA-AA 2011）とバイオマーカー

重ねられて[16]，ADの初期病態研究に新たな境地を切り開いた．^{11}C-PiBは，半減期約20分の放射性同位元素［^{11}C］で標識されているため，検査を実施するためには，院内サイクロトロンおよび合成装置のハードと，製造および品質管理のソフトを併せ持つことが必要で，普及には大きな壁がある．現在わが国に約300あるPET施設のうち，^{11}C-PiB検査が実施可能な施設はわずか20施設程度にとどまる．半減期の長い［^{18}F］で標識したアミロイドイメージング診断薬が開発され，供給体制が整えば，現在腫瘍診断に広く用いられている^{18}F-FDG（^{18}F-fluorodeoxy glucose）と同様，PET撮影装置さえあれば，アミロイドイメージング検査が実施可能となる．これまで^{18}F-florbetaben（BAY94-9172），^{18}F-flutemetamol（GE-067），^{18}F-florbetapir（AV-45）の第Ⅲ相試験が実施された．3薬のうちAV-45は北米のAD観察研究ADNI-2においても採用されるとともに，2012年4月にはいち早くFDAの承認を受けた．3薬についてはこれまで臨床研究や治験の結果が論文として発表されているが[26,32,33]，その性質はよく似ており，集積の特性も^{11}C-PiBの結果ともよく相関し，十分な実用性があると期待される．ただし，これら3薬は^{11}C-PiBと比べて白質への非特異的集積が多いので，灰白質における早期の少量の特異集積を検出する感度がやや低いのではないかといわれている．最近開発されたAZD4694（Nav4694）はこの点を改善した特徴をもつアミロイドイメージング診断薬として期待されており[6]，^{11}C-PiBとほぼ同等の集積特性を有しているといわれる[27]．

Ⅱ．アミロイドイメージング臨床研究の進展

ADと臨床診断された患者におけるアミロイドPET所見は，おおむね9割以上の陽性率が報告されている[13,16]．AD患者における陰性所見は，

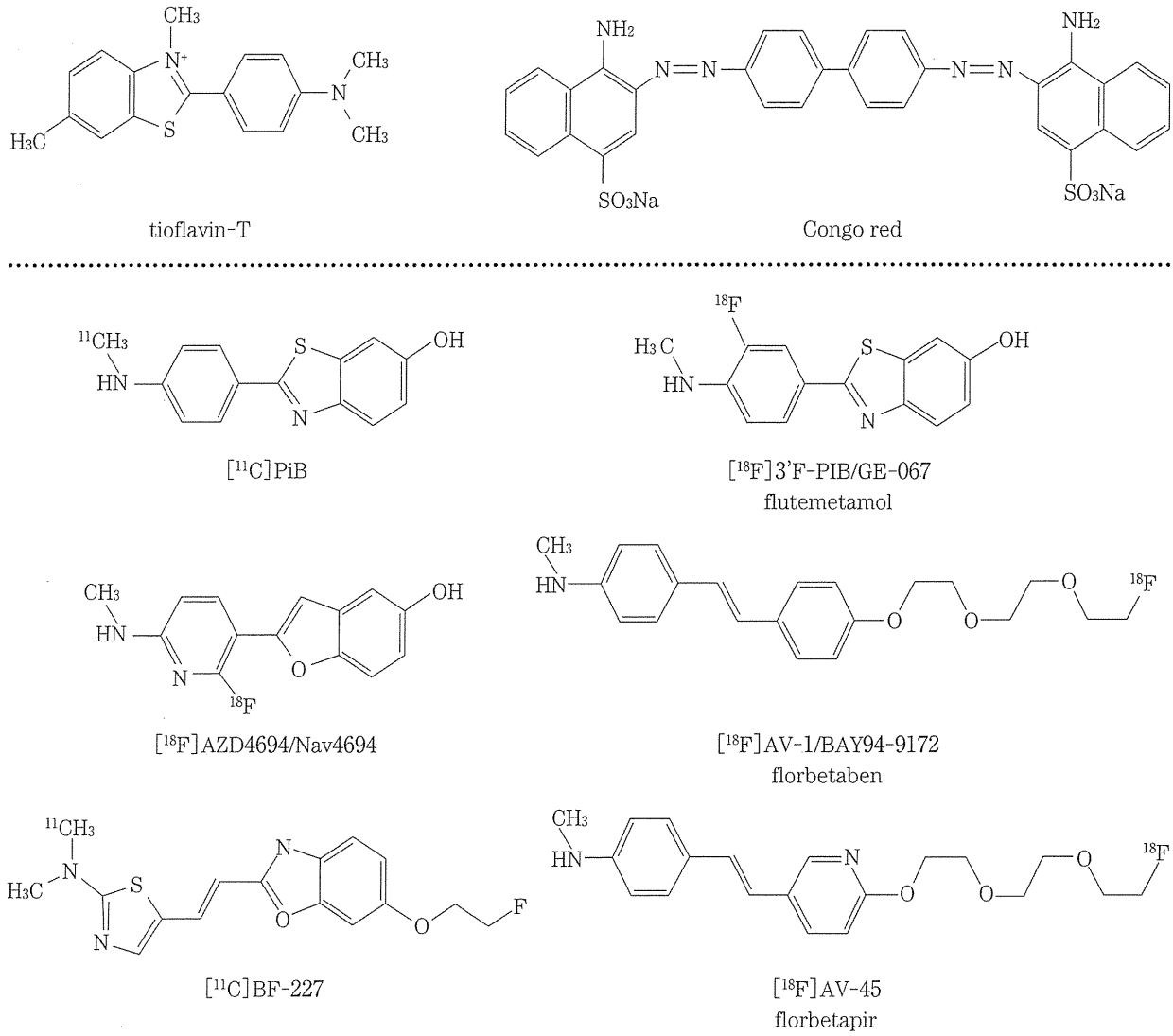

アミロイド組織染色に用いられている色素であるコンゴーレッドやチオフラビンTの類似化合物が多く用いられている．

図2　代表的なアミロイドPET診断薬

むしろ臨床診断基準による偽陽性（誤診）を検出していると考えられている．アミロイドPET陰性であるがADである症例が存在する可能性は，否定はできないが現実的にはきわめてまれであろうと考えられている．Aβに対する脆弱性の高い個体において，アミロイドPETの検出閾値が病的集積のレベルを上回ってしまう可能性，コンフォメーションの違いにより^{11}C-PiB結合能が低いアミロイドが集積するADが存在する可能性，アミロイド構造を形成しにくい変異型Aβの関与するAD[31]などが想定される．

アミロイドPETでみたAβの脳内集積は，前頭葉，楔前部および後部帯状回でとくに高く，側頭頭頂葉の外側部，線条体がこれに次ぎ，後頭葉や一次運動感覚野では相対的に低い[13,16]（図3）．この分布は剖検脳の病理学的検索で認められるAβの脳内集積の分布[4]とおおむね一致している．

Aβの沈着がAD脳でなぜこのような分布をとるのかについてはまだよくわかっていない．脳の部位によるsynaptic reserveの違い，default mode network（DMN）と呼ばれる安静時局所脳活動との関連[5]，脳局所における遺伝子発現の違い，可

溶性 Aβ と線維型 Aβ の分布の違い，老人斑と神経原線維変化の分布の違いなどに基づいた仮説の構築が試みられている．

Aβ 沈着と認知機能の指標，あるいは局所脳糖代謝や脳萎縮との相関は予想されたほど必ずしも明瞭ではない[13,16,25]．Aβ 沈着から神経細胞障害そして認知機能障害の発症に至るまでには，複雑な物質的プロセスが介在し長い時間を要するので，上流と下流の現象に同時的な相関が見いだしにくいというのが一つの解釈である．それゆえ，アミロイド PET は臨床症状進展の指標としては適切ではなく，AD 発症前に潜行する Aβ 蓄積のイベントを感度よく検出するマーカーとして考えられるようになった．

軽度認知障害（mild cognitive impairment ; MCI）における ^{11}C-PiB 検査結果は多数報告されているが，多くが 60～70% 程度の陽性率を報告している[13,15,25]．MCI 症例の ^{11}C-PiB 集積量は，AD と同等レベルか健常者と同等レベルのおおむね 2 群に別れ，その中間は少ない．このことは，Aβ 沈着が MCI の段階でほぼプラトーに達していることを示唆している．また，アミロイド PET 陽性を呈する MCI は高率に AD に移行することも指摘されている[10,17]．

さらに，健常高齢者でも，10～30% の陽性者が存在することが一貫して報告されている[13,16,21,22]．これは，従前の死亡時に認知機能正常であった高齢者における病理学的検索において，30% 前後で Aβ 沈着が認められるという報告とよく一致する[3,23]．

アポリポタンパク E（apolipoprotein E ; ApoE）ε4 型は AD の最も強いリスクとして知られているが，ApoE4 保有者では非保有者に比べてアミロイド PET 陽性率や集積量が高いことも明らかになり[24]，ApoE4 はアミロイド蓄積を促進することにより AD のリスクとなることが示唆された．

^{11}C-PiB 集積は髄液 $A\beta_{1-42}$ 濃度と逆相関の関係にあることをワシントン大学のグループが報告し[7]，その後多くのデータにより追認され，この両者が脳内 Aβ 沈着のマーカーとしておおむね同等の意義があることもわかった．

Ⅲ．新しいアルツハイマー病診断基準とアミロイドイメージング

このような臨床研究の成果を基盤として，AD の臨床診断基準として広く用いられてきた

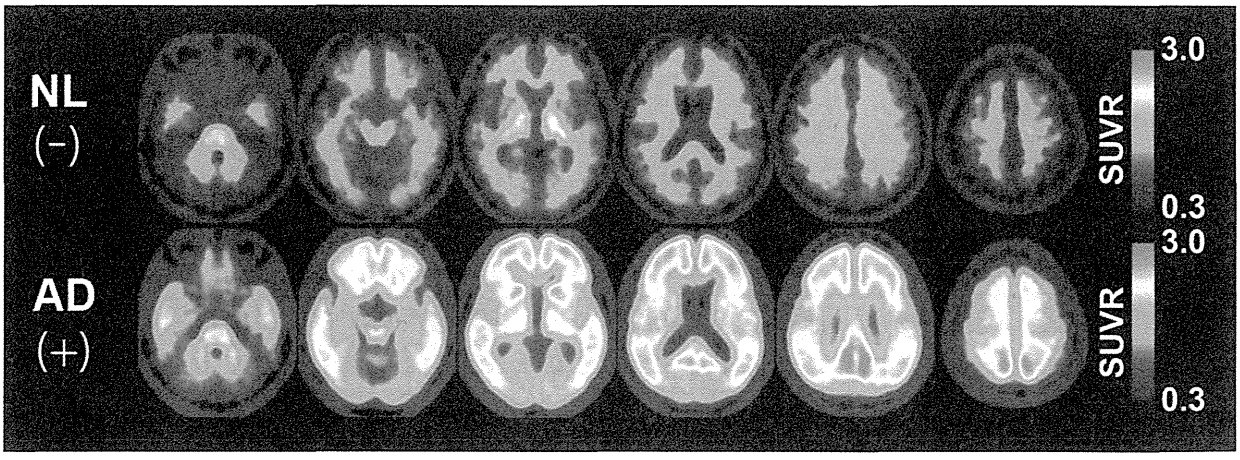

上段：集積のない健常者（陰性画像 10 例の平均），下段：集積のあるアルツハイマー病患者（陽性画像 10 例の平均）．^{11}C-PiB 投与後 40 ～ 60 分に撮影した画像における集積を，小脳皮質への集積により基準化して表示した．陰性画像では大脳白質，視床，小脳髄質，脳幹部に非特異的な少量の集積がみられるが灰白質への集積は少ない．陽性画像では灰白質とくに前頭葉，楔前部・後部帯状回，側頭葉，頭頂葉，線条体腹側部への集積が白質への非特異的集積を大きく上回る．

図 3　^{11}C-PiB によるアミロイドイメージング

NINCDS-ADRDA診断基準（1984）[19]がアメリカ国立老化研究所（National Institute on Aging；NIA）とアルツハイマー病協会（Alzheimer's Association；AA）により27年ぶりに改訂された[1,20,30]．NIA-AA 2011基準では，これまでのようにADを認知症に至って初めて発症する臨床疾患としてではなく，Aβの脳内沈着に始まり，無症候期から長い複雑なプロセスを経て最終的に神経細胞障害とその結果としての認知症に至る疾患として定義し直された．診断基準を病期により3段階に分け，Alzheimer's disease dementia（アルツハイマー病性認知症），mild cognitive impairment due to Alzheimer's disease（アルツハイマー病による軽度認知障害），preclinical Alzheimer's disease（臨床前期アルツハイマー病）とし，バイオマーカー（髄液$A\beta_{42}$，タウ〈tau〉，p-tau，MRI，FDG-PET，アミロイドイメージング等）がそのなかに組み込まれたことが大きな特徴である（図1）．バイオマーカーは，Aβの脳内沈着を示すマーカーと，機能変化と形態変化の両者を含有したかたちの細胞障害を示すマーカーの2つに区分された（表1）[1]．アミロイドイメージングは髄液$A\beta_{42}$と並び，前者のマーカーとして位置づけられている．臨床症状のあるAD dementiaやMCI due to ADでは，中核的な臨床症状に加え，バイオマーカーの検査結果が得られれば，それらに基づいて診断の確信度が加減されるかたちになっている．また，preclinical ADは認知機能正常の健常者に対する評価であり，実際にはバイオマーカーによって定義される．すなわち，Aβ沈着のバイオマーカーのみが陽性であればstage 1，神経障害のバイオマーカー陽性所見が加われればstage 2，さらに自覚的もの忘れなど，何らかの軽微な認知・行動障害が伴えばstage 3と分類する（表2）[30]．

この臨床診断基準が提案されたことにより，病態仮説に基づいたAD克服に至る道筋が明確になった．今後ADの根本治療薬の治験は，神経細胞障害の軽い，より早期の時期にシフトしていくことになろう．さらに，健常者をも対象とした発症予防に向けた臨床研究も加速している．

この臨床診断基準の実用上の問題点のひとつは，AD以外の病態とAβとの関係がまだ十分わかっていない点である．レビー小体型認知症（dementia with Lewy bodies；DLB）の病理では老人斑を伴うタイプ（common form）と伴わないタイプ

表1　アルツハイマー病診断に用いられるバイオマーカー

A．アミロイドβ沈着のバイオマーカー
　1．髄液$A\beta_{42}$
　2．アミロイドPET画像
B．神経障害のバイオマーカー
　1．髄液タウ/リン酸化タウ
　2．海馬容積（体積計測）または側頭葉内側部萎縮（視覚判定）
　3．脳萎縮速度
　4．FDG-PET画像
　5．脳血流SPECT画像

（Albert MS, DeKosky ST, Dickson D, Dubois B, et al.: The diagnosis of mild cognitive impairment due to Alzheimer's disease；Recommendations from the National Institute on Aging-Alzheimer's Association workgroups on diagnostic guidelines for Alzheimer's disease. *Alzheimers Dement*, 7：270-279, 2011）

表2　Preclinical Alzheimer's diseaseの分類

ステージ	状態の説明	Aβマーカー（PET/CSF）	神経障害マーカー（タウ，FDG，MRI）	軽微な臨床症状
stage 1	無症候性脳アミロイドーシス	陽性	陰性	なし
stage 2	無症候性脳アミロイドーシス＋神経変性の徴候	陽性	陽性	なし
stage 3	脳アミロイドーシス＋神経障害＋軽微な認知・行動障害	陽性	陽性	あり

（Sperling RA, Aisen PS, Beckett LA, Bennett DA, et al.: Toward defining the preclinical stages of Alzheimer's disease；Recommendations from the National Institute on Aging-Alzheimer's Association workgroups on diagnostic guidelines for Alzheimer's disease. *Alzheimers Dement*, 7：280-292, 2011）

(pure form) があることがKosakaら[18]によって報告されたが，アミロイドイメージングでも臨床例でこのことが確認されつつある．前頭側頭型認知症でも，健常者とおおよそ同等の頻度でアミロイド陽性者が存在することが報告されている．高齢者では複合病理の共存はまれではなく，複合病理におけるAβの存在が，単に無症候陽性者と同様なのか，併存する病理と相加／相乗効果をもった臨床的意義を有するのかの見極めが必要となる．AD以外の変性型認知症でもpreclinical stageが存在するはずであるから，このような視点をもった病態研究の展開とともに，NIA-AA 2011の実用的な適用方法を検討していく必要がある．

Ⅳ．Preclinical ADの臨床研究

Aβ沈着を認めるにもかかわらず認知機能が正常な人の脳では一体なにが起こっているのかを確認するために，無症候性アミロイド陽性者を対象とした臨床研究が最近盛んに行われており，ADの発症とその予防をめぐり近年のトピックとなっている．健常者における^{11}C-PiB陰/陽性とエピソード記憶や他の認知指標は相関があるという報告とないという報告がある．機能的MRI（fMRI）で検出したdefault mode networkの機能的相関が^{11}C-PiB陽性健常者では^{11}C-PiB陰性健常者よりも低下しており，この方法が最も早期の脳機能変化をとらえている可能性が指摘されている[29]．Morminoら[22]は，健常者における大脳への^{11}C-PiB集積量と海馬容積に逆相関があることを報告している．

これらの結果は，健常者における脳Aβ沈着と認知機能低下，脳萎縮が関連することを示唆しているが，いずれも統計学的な相関レベルは低く，やはり両者の間には介在する複数のプロセスと時間が存在することを示唆している．こうした見失われている病態プロセスの詳細を盛り込んだモデルの構築と検証が必要とされる．

Ⅴ．アミロイドイメージングと発症予防介入研究

ADは不可逆的なプロセスをたどり，患者や家族の社会生活に深刻な影響を及ぼすので，疾患克服の究極的な目標は発症予防であることはいうまでもない．ここ数年AD発症者を対象としたアミロイド制御薬の治験がことごとく期待はずれの結果に終わり，神経細胞障害プロセス（タウカスケード）がひとたび回り始めると，それは自立的に進展し，その時点でAβを取り除いても病態の進行を阻止できないのではないかと考えられるようになった．この点からも，AD発症者に対して効果がなかったアミロイド制御薬を，より早期の段階で，望むらくは発症前のリスク保有者に適用し，発症遅延あるいは阻止ができるかどうかを検討する臨床研究の必要が検討されるようになった．

健常者を対象とした介入研究は，多数の被験者をエントリーする必要があること，介入による健康被害の可能性があること，追跡が長期に及ぶことなど，多くの困難な問題を抱えている．こうしたなかで，常染色体優性遺伝型の家族性アルツハイマー病を対象とした追跡介入研究のプロジェクトが立ち上げられ，未発症キャリアに対する薬物介入により，発症遅延が可能かを検証しようとしている．そのひとつはワシントン大学（セントルイス）を中心とするDominant Inherited Alzheimer Network（DIAN）研究で，対象となる常染色体優性型のADはアミロイド前駆体タンパク（APP），プレセニリン-1（PS1），PS-2変異例で，保因者は平均43歳でADを発症し，浸透率は8割とされており，未発症者への薬物介入による発症遅延を試みる十分な倫理的基盤があると考えられている．アリゾナ大学のReimanらは，コロンビアの優性遺伝アルツハイマー病家系（presenilin-1 E280A）に属する約300人を対象とした観察および介入研究Alzheimer's Disease Prevention Initiative（API）研究をスタートさせた．

これらの常染色体優性遺伝型ADは，高齢者に